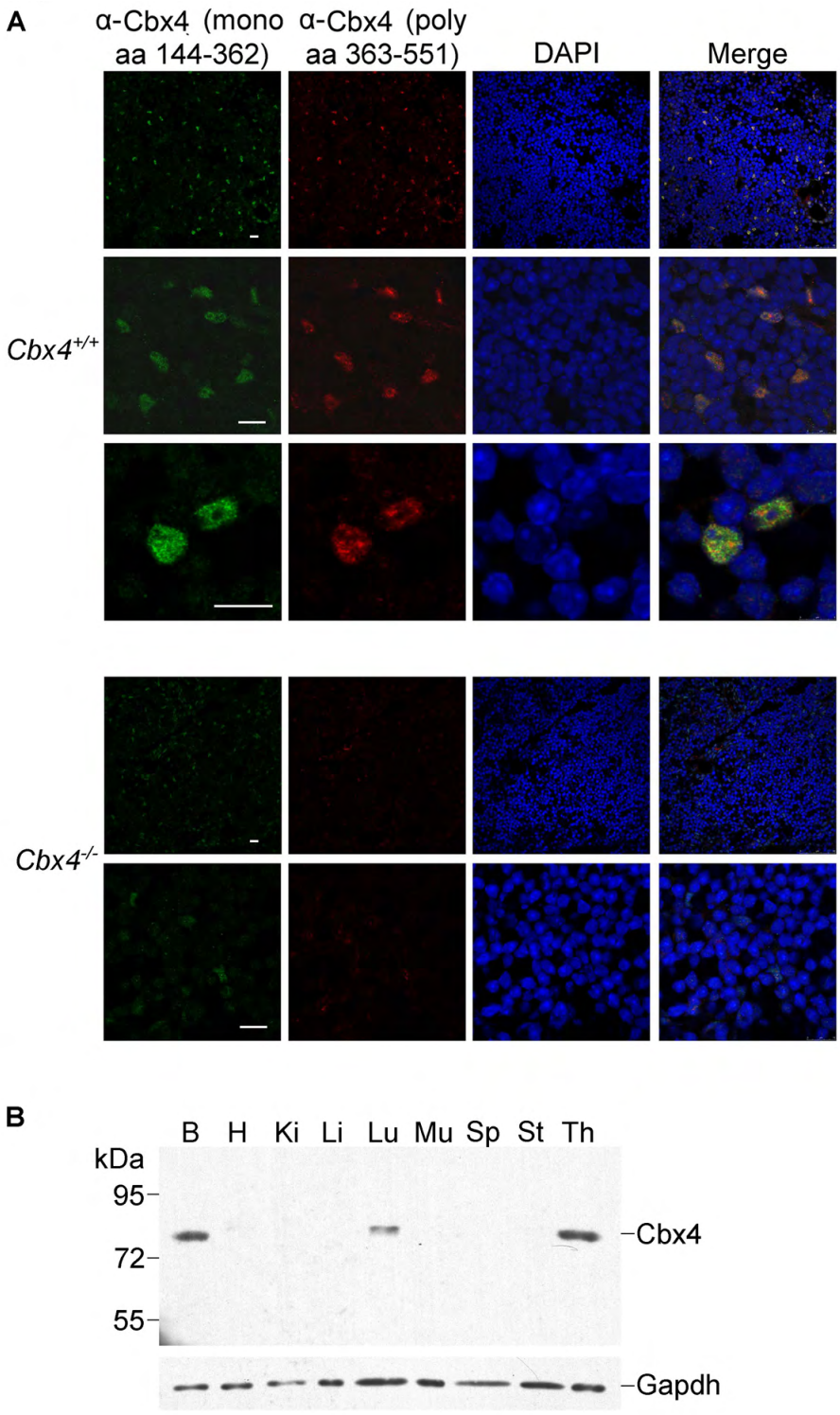

Fig. S1. Cbx4 protein expression in mouse tissues. (**A**) Validation of the specificity of Cbx4 antibodies. Immunostaining of thymic sections from wild-type (+/+) and Cbx4-deficient (–/–) E17.5 embryos was carried out to assess the performance of a mouse monoclonal antibody raised against amino acids 144-362 and a rabbit polyclonal antibody against amino acids 363-551. Scale bars: 10 μm. (**B**) Cbx4 protein expression in newborn mouse tissues. Total cellular lysate was prepared from various tissues of newborn mice and resolved on a SDS-PAGE. The blot was probed with a polyclonal antibody against C-terminal region of Cbx4. Gapdh served as a loading control (bottom panel). B, brain; H, heart; Ki, kidney; Li, liver; Lu, lung; Mu, skeletal muscle; Sp, spleen; St, Stomach; Th, thymus.

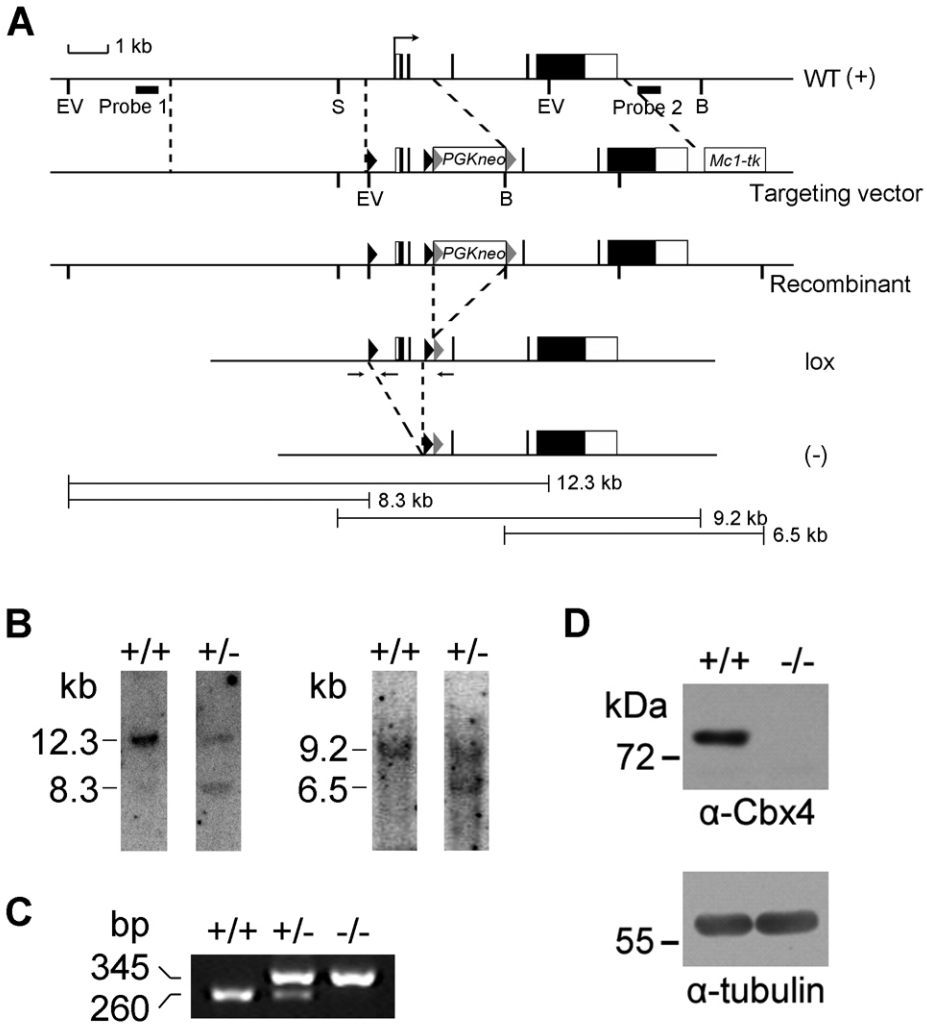

Fig. S2. Targeted disruption of Cbx4. (**A**) Knockout strategy of the *Cbx4* gene. Coding exons are indicated as filled boxes and untranslated regions as blank boxes. *Lox*P sites are shown as black triangles and Frt sites as hatched triangles. The floxed region contains exons 1 and 2, which code for the major part of the chromo domain. Probes used to identify recombinant ES cells are shown as horizontal bars and the PCR primers for genotyping as arrowheads. Restriction sites involved in Southern analysis are *Eco*RV (EV), *Bgl*II (B) and *Sal*I (S). (**B**) Genotyping of a selected ES clone by Southern blotting using probe 1 (left) and probe 2 (right) as indicated in A. (**C**) PCR genotyping of Cbx4-deficient mice. (**D**) Loss of the Cbx4 protein in homozygous mutant mice was confirmed by western blotting. Tubulin served as a loading control.

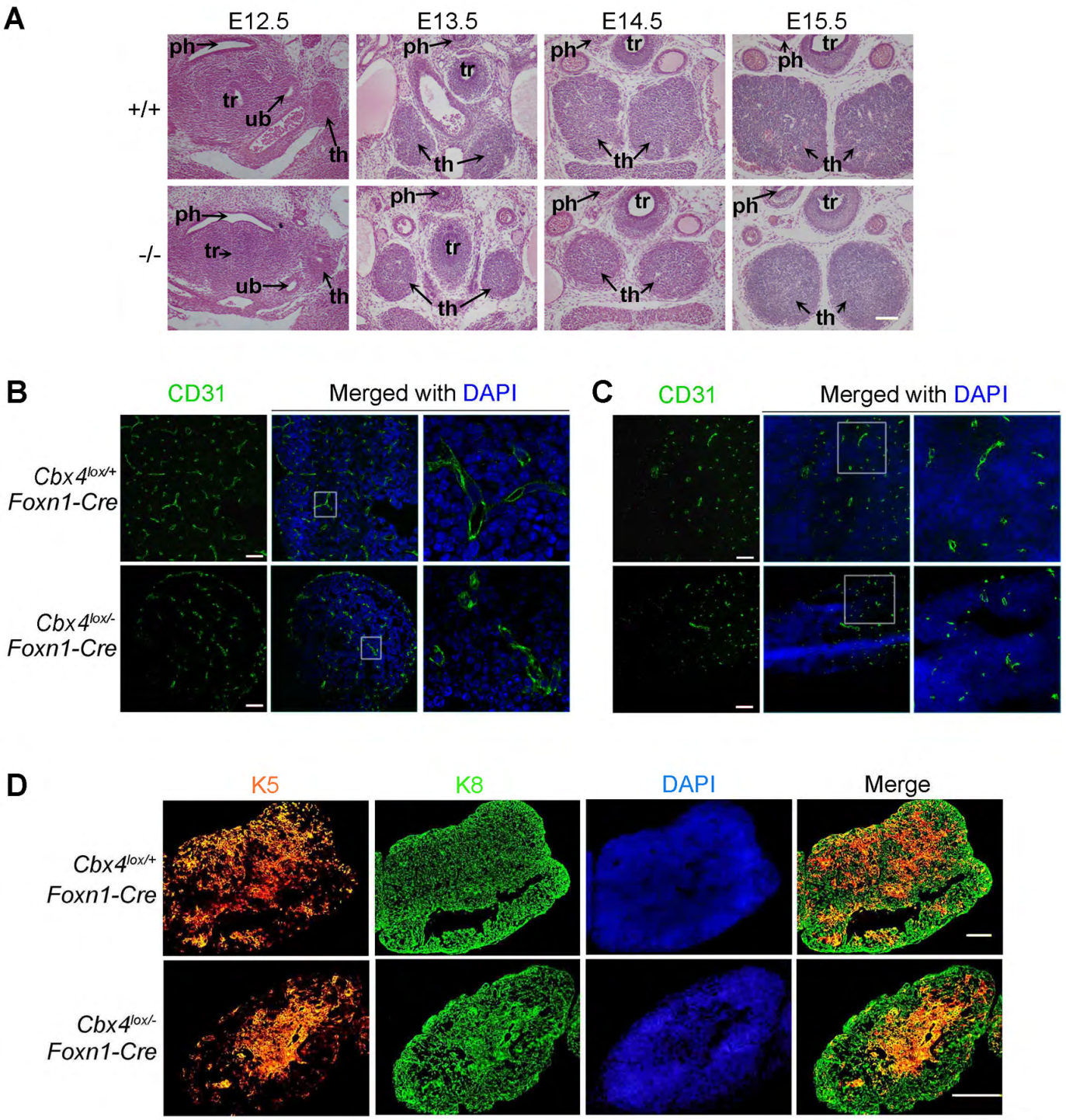

Fig. S3. Structure of the thymus with the disruption of Cbx4. (**A**) Histological abnormalities in the Cbx4-deficient thymi during embryonic development. Transverse sections were prepared from E12.5 to E15.5 embryos followed by Hematoxylin and Eosin staining. The dorsal side is upwards. ph, pharynx; tr, trachea; th, thymus; ub, ultimobranchial body rudiment. Scale bar: 100 μm. (**B**,**C**) Immunostaining of CD31 in E18.5 (B) and 2-week-old (C) [*Cbx4*$^{lox/+}$, Foxn1-Cre] and [*Cbx4*$^{lox/-}$, Foxn1-Cre] thymi. The squares in the middle panel were magnified to generate the images in the right panel. Scale bars: 60 μm. (**D**) E18.5 thymic sections were stained for the medullary epithelial marker K5 and cortical epithelial marker K8. Scale bar: 200 μm.

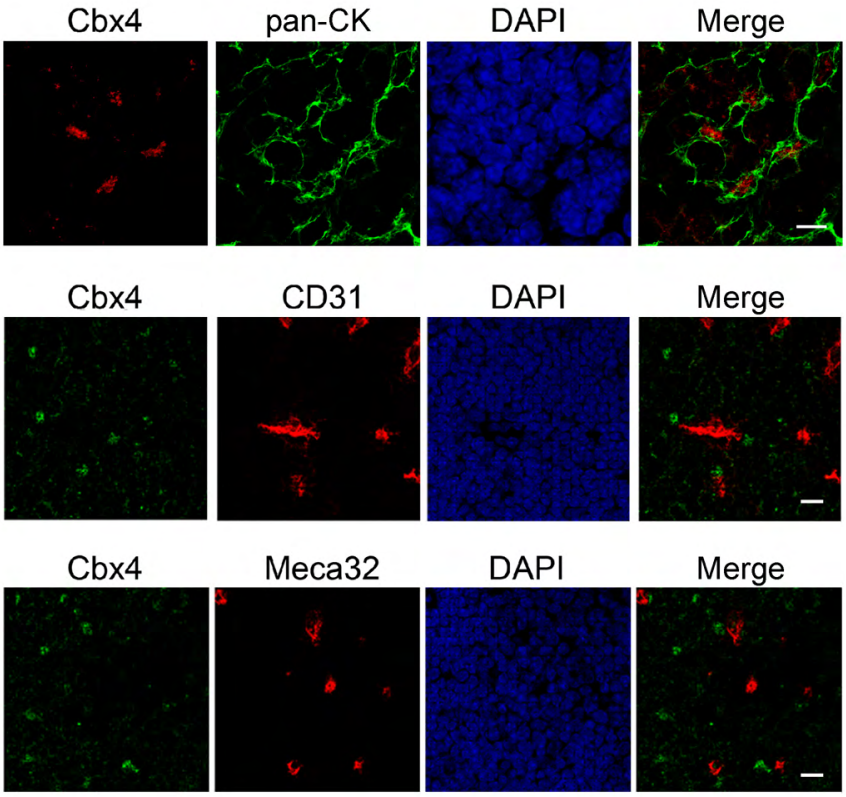

Fig. S4. Lack of Cbx4 protein expression in thymic endothelial cells. E18.5 thymic sections were co-stained with anti-Cbx4 and antibodies for the epithelial marker pan-CK or the endothelial markers CD31 and Meca32. Scale bars: 10 μm.

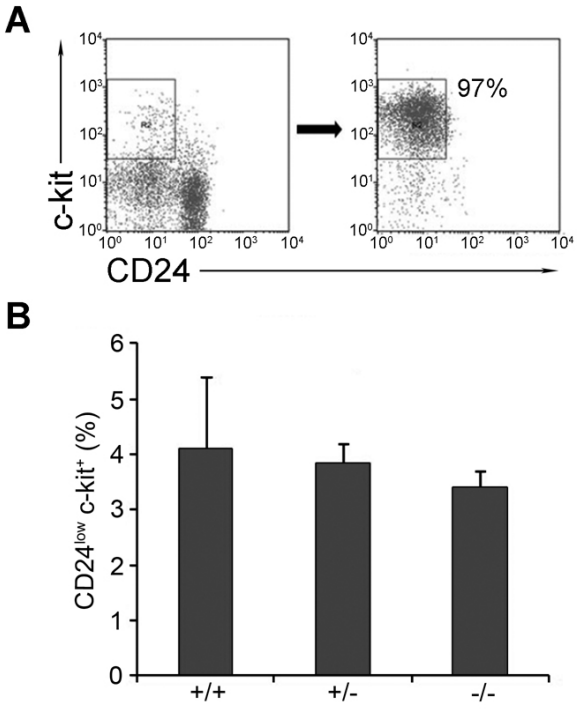

Fig. S5. Unaltered production of HPCs in E15.5 *Cbx4*$^{-/-}$ fetal liver. (**A**) Enrichment of CD24^{low}c-kit^{+} cells (HPCs) from E15.5 fetal livers by flow cytometry. The number given denotes the purity of enriched HPCs. (**B**) Percentage of HPCs in the fetal liver cells of E15.5 *Cbx4*$^{+/+}$, *Cbx4*$^{+/-}$ and *Cbx4*$^{-/-}$ embryos. $n \geq 3$.

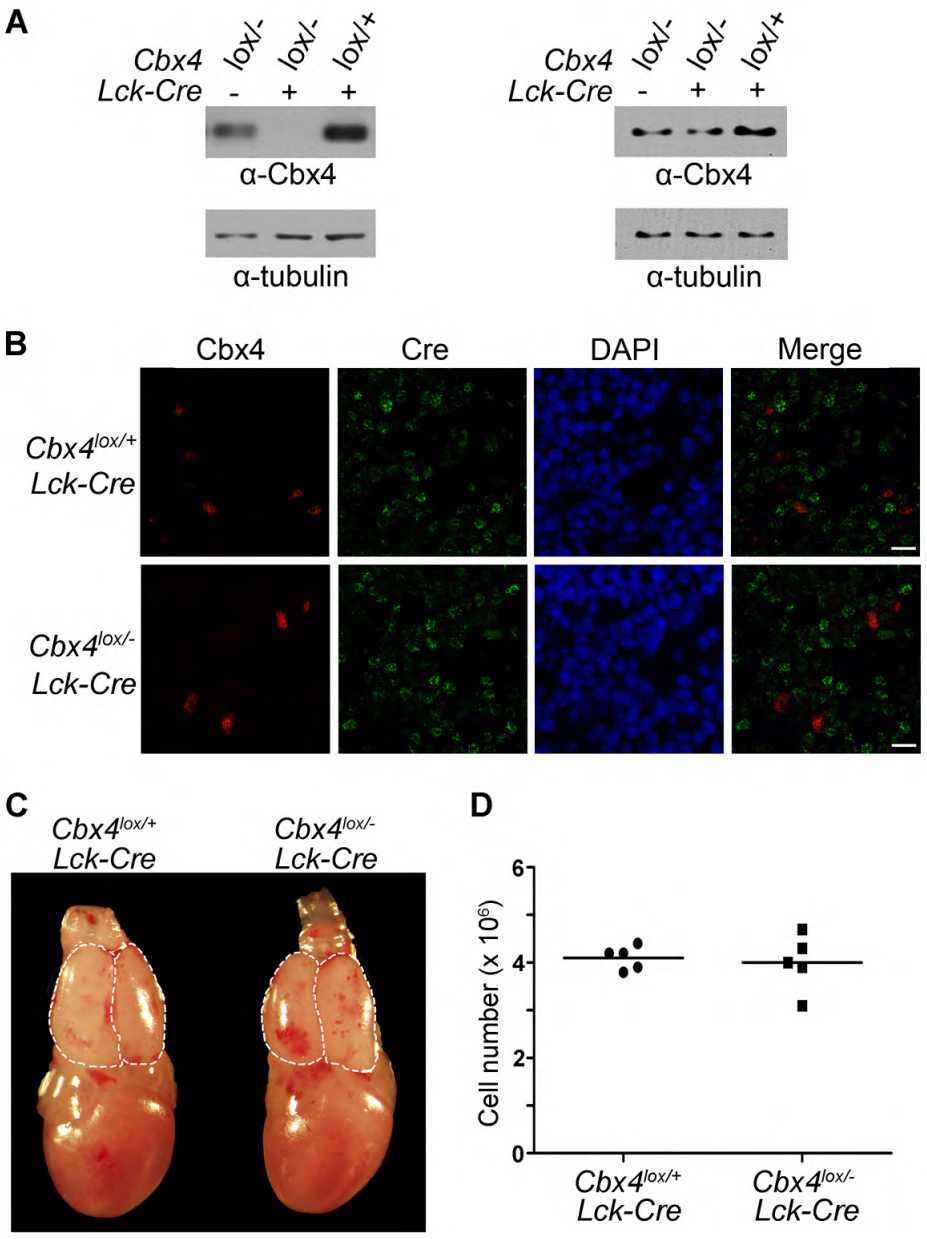

Fig. S6. Thymocyte-specific disruption of Cbx4 by breeding with Lck-Cre mice. (**A**) Cbx4 protein expression was lost in thymocytes (left) but maintained in the brain (right) of [*Cbx4*$^{lox/-}$, Lck-Cre] mice. Tubulin served as a loading control. (**B**) Mutually exclusive staining of Cbx4 and Cre in E17.5 thymi. Scale bar: 10 μm. (**C**) Gross appearance of thymi with thymocyte-specific deletion of *Cbx4*. Representative images of thymi from [*Cbx4*$^{lox/+}$, Lck-Cre] and [*Cbx4*$^{lox/-}$, Lck-Cre] newborn mice are shown. (**D**) The total number of thymocytes in [*Cbx4*$^{lox/+}$, Lck-Cre] versus [*Cbx4*$^{lox/-}$, Lck-Cre] newborn mice. Each dot represents an individual sample and horizontal bars indicate the mean. n=5.

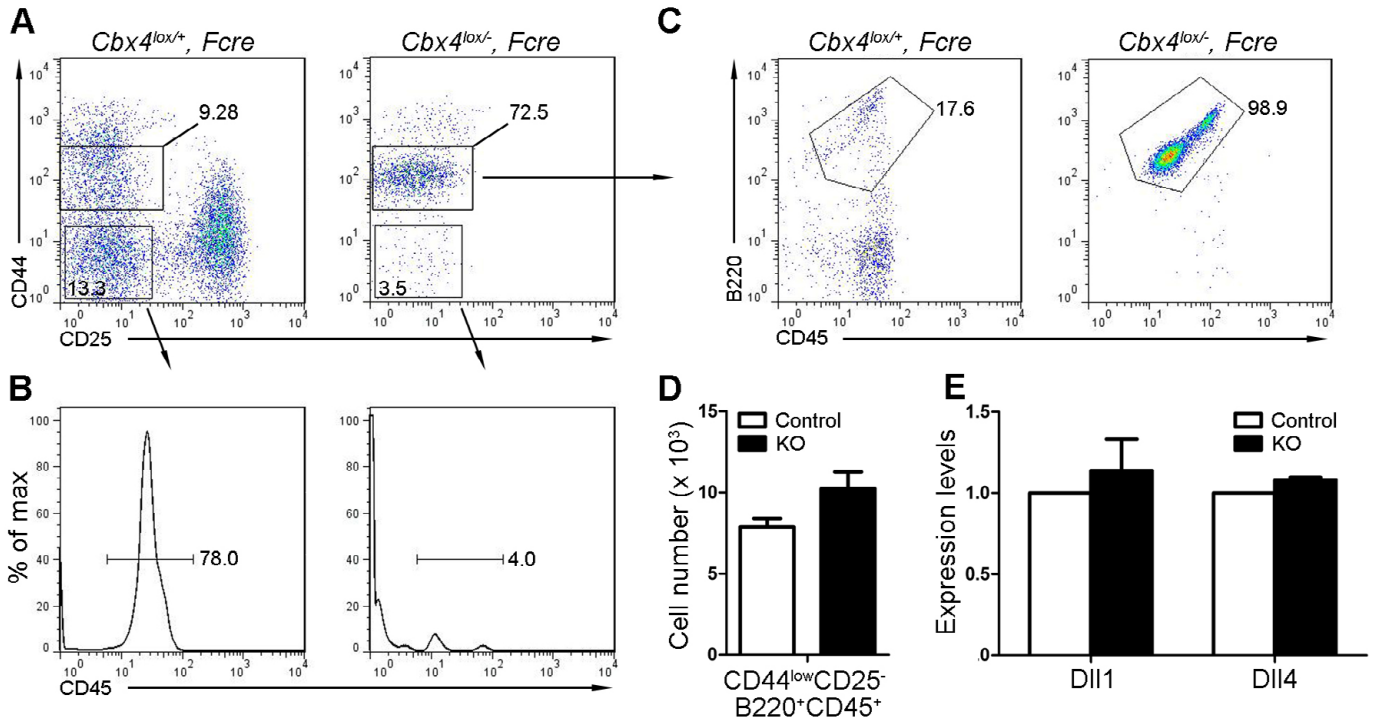

Fig. S7. Analysis of DN subsets in the thymi of 3-week-old [*Cbx4*$^{lox/-}$, Foxn1-Cre] mice. (**A**) Ter119$^-$CD4$^-$CD8$^-$ cells were analyzed by their CD44/CD25 pattern. The numbers indicate the percentage of the CD44^{low}CD25$^-$ and CD44$^-$CD25$^-$ subsets, respectively. (**B**) CD44$^-$CD25$^-$ cells were further analyzed by the expression pattern of CD45, and the numbers indicate the percentage of CD45-positive cells. (**C**) CD44^{low}CD25$^-$ cells were further analyzed by the expression pattern of CD45 and B220, and the numbers indicate the percentage of B-lineage cells. (**D**) Quantification of Ter119$^-$CD4$^-$CD8$^-$ CD44^{low}CD25$^-$B220$^+$CD45$^+$ cells in each thymic lobe. Absolute cell numbers were calculated as (cell frequency × total number of thymic cells). (**E**) Relative mRNA levels of Delta-like 1 and Delta like 4 in the whole thymi were analyzed by quantitative PCR. *n*=3.

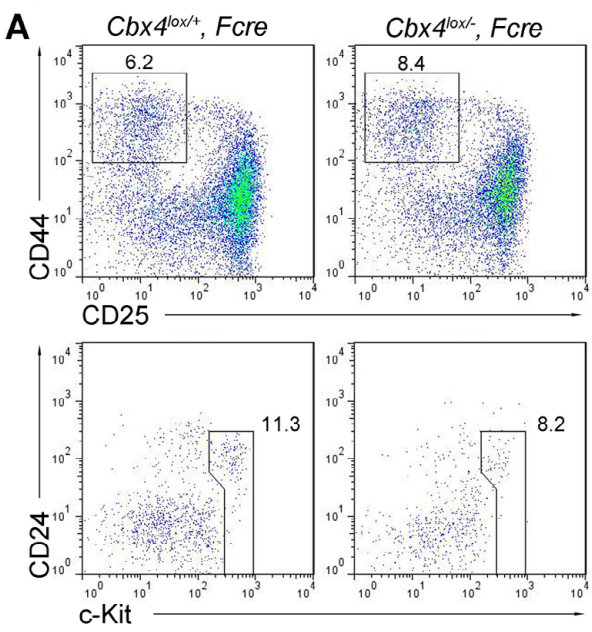

Fig. S8. Early thymic progenitors in the thymi of newborn [*Cbx4*$^{lox/-}$, Foxn1-Cre] mice. Ter119$^-$CD4$^-$CD8$^-$ CD44$^+$CD25$^-$ cells as indicated in the boxed regions in the upper panels were further identified by their pattern of Kit and CD24 expression as shown in the lower panels. The boxed regions in the lower panels indicate ETPs; the numbers indicate the percentage of cells in those boxed areas.

Table S1. Primers used for RT-PCR

Gene	Forward primer (5′-3′)	Reverse primer (5′-3′)
β-actin	GAAATCGTGCGTGACATCAAAG	TGTAGTTTCATGGATGCCACAG
Bmp2	GGGACCCGCTGTCTTCTAGT	TCAACTCAAATTCGCTGAGGAC
Bmp4	GAGGGATCTTTACCGGCTCC	GTTGAAGAGGAAACGAAAAGCAG
Bmpr1	GCTTGCGGCCAATCGTGTCTAA	GCAGCCTGTGAAGATGTAGAGG
Bmpr2	TTGGGATAGGTGAGAGTCGAAT	TGTTTCACAAGATTGATGTCCCC
Ccl19	GGGGTGCTAATGATGCGGAA	CCTTAGTGTGGTGAACACAACA
Ccl21	GCTGCCTTAGTACAGCCAG	GTGTCTGTTCAGTTCTCTTGC
Ccl25	AGTGTGTGGGAATCCAGAGGA	CGCTTGTACTGTTGGGGTTCT
CD80	ACCCCCAACATAACTGAGTCT	TTCCAACCAAGAGAAGCGAGG
CD86	TGTTTCCGTGGAGACGCAAG	TTGAGCCTTTGTAAATGGGCA
Chordin	TCCAGAGCATCGCAGTTACAG	AGAGAAGCGTAAACTTGAGCG
Cxcl10	TTTCTGCCTCATCCTGCTG	TCGTGGCAATGATCTCAACA
Cxcl11	GGAAGGTCACAGCCATAGCC	GTCCAGGCACCTTTGTCGTT
Cxcl12	TGCATCAGTGACGGTAAACCA	TTCTTCAGCCGTGCAACAATC
K14	AAGGTCATGGATGTGCACGAT	CAGCATGTAGCAGCTTTAGTTCTTG
Dll 1	CAGGACCTTCTTTCGCGTATG	AAGGGGAATCGGATGGGGTT
Dll 4	CAGTTGCCCTTCAATTTCACCT	AGCCTTGGATGATGATTTGGC
Fgf10	GACCAAGAATGAAGACTGTCCG	TACAGTCTTCAGTGAGGATACC
Fgf7	GCGCAAATGGATACTGACACG	GGGCTGGAACAGTTCACACT
FgfR2IIIb	CCCATCCTCCAAGCTGGACTGCCT	CAGAACTGTCAACCATGCAGAGTG
Gapdh	GCCAGCCTCGTCCCGTAGACA	CAACAATCTCCACTTTGCCACTGC
Noggin	CATGCCGAGCGAGATCAAAG	CTGCCCACCTTCACGTAGC

Tsg	TCTAGCCTCCCTGACGTTCC	CACATACCGACACAGTCGC